

U.S. DEPARTMENT OF COMMERCE/Environmental Science Services Administration



Technical Report

INSTITUTES FOR ENVIRONMENTAL RESEARCH IER 6-ITSA 6

A Method of Measuring the Multipath Components of a Field

C. C. WATTERSON

AUGUST, 1966

Boulder, Colorado

THE INSTITUTES FOR ENVIRONMENTAL RESEARCH

The mission of the Institutes is to study the oceans, and inland waters, the lower and upper atmosphere, the space environment, and the earth, seeking the understanding needed to provide more useful services. These research Institutes are:

- The Institute for Earth Sciences
conducts exploratory and applied research in geomagnetism, seismology, geodesy, and related earth sciences.
- The Institute for Oceanography
works to increase knowledge and improve understanding of the ocean and its interaction with the total physical environment of the globe.
- The Institute for Atmospheric Sciences
seeks the understanding of atmospheric processes and phenomena that is required to improve weather forecasts and related services and to modify and control the weather.
- The Institute for Telecommunication Sciences and Aeronomy
supports the Nation's telecommunications by conducting research and providing services related to radio, infrared, and optical waves as they travel from a transmitter to a receiver. The Institute is also active in the study and prediction of periods of solar activity and ionospheric disturbance.

Environmental Science Services Administration

Boulder, Colo.



U. S. DEPARTMENT OF COMMERCE

John T. Connor, Secretary

ENVIRONMENTAL SCIENCE SERVICES ADMINISTRATION

Robert M. White, Administrator

INSTITUTES FOR ENVIRONMENTAL RESEARCH

George S. Benton, Director

ESSA TECHNICAL REPORT IER 6-ITSA 6

A Method of Measuring the Multipath Components of a Field

C. C. WATTERSON

INSTITUTE FOR TELECOMMUNICATION SCIENCES AND AERONOMY
BOULDER, COLORADO
August, 1966

For sale by the Clearinghouse for Federal Scientific and Technical Information
Springfield, Virginia 22151 - Price \$2.00

CONTENTS

	Page
1. Introduction -----	1
2. Description of the Method -----	2
3. Analysis of the Method -----	6
3.1. Solutions for One Axis and Antenna Orientation -----	6
3.2. Matching and Averaging of Multiple Solutions -----	10
3.3. Combined Solution -----	15
3.4. Rotation of the Coordinate System -----	22
4. Discussion -----	24
5. Experimental Results -----	28
6. Conclusions -----	31
7. References -----	33

FOREWORD

This work was supported by Rome Air Development Center, Griffiss Air Force Base, New York, under contract AF30(602)-2385.

ABSTRACT

A description and analysis is presented of a method of making field-strength measurements in a multipath field from which computations can be made of the amplitude, phase, and angle of arrival of each of a number of coherent elliptically-polarized plane-wave multipath components. The method requires that the amplitude and phase of the received signal from a moving dipole or other small-aperture antenna be measured as the antenna is moved successively along three orthogonal straight-line paths.

The dynamic range of the amplitude of the multipath components which can be measured is approximately equal to the ratio of the amplitude of the strongest component to the magnitude of the errors of measurement. The angular resolution is approximately equal to the beamwidth of an antenna whose aperture equals the distance of movement of the dipole. The errors in the solutions are least for the strongest multipath components and greatest for the weaker components. In a computer evaluation which used measurements of two-figure accuracy, the stronger component errors were less than one-tenth of a dB in amplitude, several tenths of a degree in phase and about one-tenth of a degree in angle of arrival. Measurements of an actual multipath field have demonstrated the practicality of the technique.

A Method of Measuring the Multipath Components of a Field

C. C. Watterson

1. Introduction

If field-strength measurements are made of an electromagnetic field composed of a single plane wave, reasonably accurate and meaningful measurements can be obtained. However, over a large portion of the spectrum, particularly above the HF region, the radiated electromagnetic field of a transmitting source at any point in the far field is usually not due to a single plane wave, but consists of multipath components caused by wave reflection and diffraction from the terrain, buildings, and other objects. Conventional field-strength measurements made under these conditions can vary considerably with a relatively small change in the position of measurement [Cottony, 1958]. The variation is caused by the fact that the total field at any point, which is the vector sum of all multipath components, changes due to the variation in the relative time phases of the multipath components. Simple field-strength measurements that are made in a multipath field, therefore, will not yield sufficient information to adequately describe the field for many applications.

One approach to solving this problem is to individually measure the amplitude, polarization, direction of arrival, and relative time phase of each multipath component. The most direct method of doing this would be to use a measuring antenna with a narrow beam that can receive one component at a time while rejecting all others. Portable antennas of sufficiently small beamwidth can be impractical in the UHF region and lower, however, making a technique which relies on small-aperture antennas desirable.

A method was developed by Hamlin, et al. [1949] and Brooks [1951] for measuring the amplitude, elevation angle of arrival, and relative time phase for each of two horizontally-polarized multipath components in a common vertical plane (a direct wave and its ground reflection). Three vertically-spaced dish antennas were used at 9.3 Gc/s and excellent angular resolving power was obtained. However, since the method is limited to two linearly polarized multipath components arriving in a common vertical plane, it is not applicable to the more general case of a larger number of multipath components of differing non-linear polarizations arriving from any direction.

Since a technique had not previously been devised for measuring the components of a multipath field where the number of components, their polarizations, and directions of arrival are unrestricted, the method to be described was devised. A brief summary of the method has been presented earlier [Watterson, 1962]. The general approach is the same as that used by Ryle [1957, 1960] for synthesizing a large-aperture antenna from a series of measurements with two small-aperture antennas. It differs principally in that it is applicable to the measurement of discrete coherent multipath components, whereas Ryle's technique is used for diffuse incoherent cosmic noise sources.

2. Description of the Method

The assumptions which are made in this method of measuring a multipath field are (a) that each of the multipath components is an essentially discrete elliptically-polarized plane wave whose direction of arrival does not change appreciably over the volume of measurement, (b) that the field does not change during the time of measurement, and (c) that the field is produced by a CW signal or a signal with a CW

component. From a series of measurements using a small-aperture, large-beamwidth antenna, it is possible to determine seven quantities for each multipath component: the amplitude and relative time phase of the horizontal electric field component, the amplitude and relative time phase of the "vertical" electric field component (normal to the horizontal component and the direction of propagation), the azimuth and elevation angles of arrival at the measuring site, and the rate of attenuation of the component with distance.

The equipment arrangement and how it is used for making the field-strength measurements is illustrated in fig. 1. Two antennas are used, both of which feed a calibrated receiver whose output is fed to a recorder. During the entire course of the measurements, the first antenna, a dipole or any other type, is located at any convenient fixed position. Its function is to provide a signal, V_a , to be used as a phase reference. The second antenna, a dipole, is mounted on a motor-driven carriage that moves along a simple portable track which provides straight-line guidance for the antenna movement. The movement of the recorder chart or tape is synchronized with that of the second antenna along its track, so that the output of the receiver is plotted as a function of the distance of movement of the second antenna.

As illustrated in fig. 1, the track which guides the movement of the second antenna is consecutively positioned in three mutually perpendicular directions so that the movement of the second antenna for each track position defines an axis of a Cartesian coordinate system x-y-z. During the measurements along each axis, the orientation (or polarization) of the second antenna is made to have up to three orthogonal values where the dipole axis is parallel to the x, y, and z axes. Since three axes of measurement and three antenna orientations are used, there are nine combinations of antenna orientation and axis of measurement possible. A minimum of

five of these combinations must be used and, for practical reasons, it is desirable to use all nine.

For each antenna orientation that is used on each axis measurement, it is necessary to determine the amplitude of the signal from the second antenna, V_b , and its time phase, ϕ , relative to the phase of the signal, V_a , from the first antenna, as a function of the distance of movement of the second antenna. The most desirable method of doing this is to have a receiver that directly measures these quantities for recording.

From the measurements which are made of the amplitude and phase of the signal from the second antenna it is possible to calculate the desired seven quantities for each multipath component. Before analyzing the method of calculation, a consideration of the relationships between the multipath field components and the measured quantities of signal amplitude and phase is desirable. The pattern which is used in assigning subscripts and superscripts is as follows: prime, double-prime, and triple-prime superscripts are used to indicate that the orientation of the second antenna is parallel to the x, y, and z axes respectively; subscripts x, y, and z are used to indicate measurements along the x, y, and z axes respectively, and numerical subscripts are used to number the multipath components, where j represents any number.

The x-y-z coordinate system defined by the lines of movement of the second antenna is illustrated in fig. 2. Let it be assumed that the x-y plane is horizontal. The line SO depicts the direction of propagation of the jth multipath component, which has an azimuthal angle of arrival α_j and the elevation angle of arrival θ_j . The angles of arrival measured with respect to the three positive axes are γ_{xj} , γ_{yj} , and γ_{zj} . The angles of arrival are the same at all points on all axes. Since the jth multipath component is in general an elliptically-polarized plane wave, it can be described in terms of the orthogonal horizontal and "vertical" electric

field components with amplitudes $E_{\alpha j}$ and $E_{\beta j}$ and phases $\theta_{\alpha j}$ and $\theta_{\beta j}$ respectively at the origin of the coordinate system. The phases are defined with respect to the signal, V_a , from the fixed first antenna.

The second antenna, whose center moves along any of the three axes, has a voltage output response to the j th multipath component which depends upon its orientation; in general it responds to spatial components of both $E_{\alpha j}$ and $E_{\beta j}$. When the axis of the second antenna, a dipole, is parallel to the x axis, the component of $E_{\alpha j}$ in the SOx plane and the component of $E_{\beta j}$ in the SOx plane add to produce E'_j to which the antenna responds. Similarly, when the dipole's axis is parallel to the y and z axes, the spatial components of $E_{\alpha j}$ and $E_{\beta j}$ in the SOy and SOz planes add to produce E''_j and E'''_j to which the antenna responds. E'_j , E''_j , and E'''_j have phases at the origin of θ'_j , θ''_j , θ'''_j .

The problem which is solved from the recordings of the amplitude and phase of the signal from the second antenna consists of obtaining a group of parallel, similar preliminary solutions, one for each combination of antenna orientation and axis of measurement that is used. For example, quantities containing E'_j , θ'_j , γ_{xj} , and σ_{xj} (an attenuation or distance-decay factor for x -axis measurements) are calculated from the amplitude and phase measurements of the signal from the second antenna which are made when it moves along and is parallel to the x axis; quantities containing E''_j , θ''_j , γ_{zj} , and σ_{zj} are calculated from the measurements along the z axis with the antenna parallel to the y axis; etc.

The results of the parallel preliminary solutions are then combined to average redundant quantities and obtain the final solutions desired for each multipath components: α_j , β_j , $E_{\alpha j}$, $E_{\beta j}$, $\theta_{\alpha j}$, $\theta_{\beta j}$, and σ_j .

3. Analysis of the Method

3.1. Solutions for One Axis and Antenna Orientation

One of the assumptions made earlier was that the direction of arrival of each of the multipath field components does not change appreciably over the distance of measurement, since the analysis being presented does not allow for such a variation. If an appreciable change in the direction of arrival of any multipath field component is not allowed over the distance of measurement, this implies that the source, or apparent (image) source, of each multipath field component is necessarily reasonably far removed from the measuring site. Consequently, the amplitude of each multipath field component does not change appreciably over the distance of measurement. Even so, it is desirable to incorporate a distance-decay factor (as the imaginary component of a complex angle of arrival) in order to handle the complex solutions for the angles of arrival which result when the sources are not sufficiently far removed, or which are introduced by errors of measurement. Since the sources or apparent sources are reasonably far removed from the measuring site, an exponential distance-decay factor is an accurate approximation to the actual inverse distance-decay.

Let it be assumed that there are n multipath components each of which produce a voltage output component in the second antenna. The following equation then can be written to describe the signal output of the second antenna when it is oriented parallel to and moving along the x axis:

$$V_b'(x) e^{i\phi'(x)} = \sum_{j=1}^n V_{xj}' e^{-\sigma'_{xj} x + i\left(\theta'_{xj} + \frac{2\pi}{\lambda} x \cos \gamma'_{xj}\right)}, \quad (1)$$

where V'_{xj} is the voltage component produced by the multipath field component E'_j and λ is the wavelength. With suitable changes in the x subscripts and variable and/or in the prime superscripts, (1) applies equally well for other axes of measurement and/or other antenna orientations. Since this is the case, the subscripts and superscripts will be dropped to simplify this portion of the analysis, and the analysis will apply to any of the nine combinations of antenna orientation and axis of measurement.

Equation (1) can be solved for the $4n$ unknown values of V_j, σ_j, θ_j , and γ_j by obtaining from the recorded measurements the values for V_b and ϕ at $2n$ or more equally-spaced points along the axis of measurement.

Let one of the points be at the origin of the coordinate system and let the distance between adjacent points be $d \leq \lambda/2$. If the points are numbered from the origin by an integer, k , then

$$x = kd \quad , \quad a \leq k \leq b. \quad (2)$$

Also, let the total number of data points be N so that

$$N = b - a + 1 \quad , \quad N \geq 2n. \quad (3)$$

Equation (1) can then be rewritten

$$M(k) = \sum_{j=1}^n p_j r_j^k \quad , \quad a \leq k \leq b, \quad (4)$$

where

$$M(k) = V_b(k) e^{i\phi(k)} \quad , \quad (5)$$

$$p_j = V_j e^{i\theta_j} \quad , \quad (6)$$

and

$$r_j = e^{i \left(\frac{2\pi d}{\lambda} \cos \gamma_j + i \sigma_j d \right)}. \quad (7)$$

Equation (4) is a set of complex non-linear simultaneous equations, one equation for each of the integral values of k , which must be solved for the unknown values of p_j and r_j . Because of the particular symmetric form of these equations, they can be solved by a variation of Prony's method [Hildebrand, 1956]. Let the solutions for $r_1, r_2, r_3 \dots r_n$ be the roots of the polynomial

$$\sum_{m=0}^n u_m r^m = \prod_{j=1}^n (r - r_j) = 0, \quad u_n = 1. \quad (8)$$

Now let the first equation in (4), for $k = a$, be multiplied on both sides by u_0 , let the second equation be multiplied by u_1 , the third by u_2 and so on to the $(n + 1)$ st equation which is multiplied by $u_n = 1$. Let these $n + 1$ modified equations be added to obtain

$$\sum_{m=0}^n M(a + m) u_m = \sum_{j=1}^n p_j r_j^a \sum_{m=0}^n u_m r_j^m = 0, \quad (9)$$

which is equal to zero because the last summation is the polynomial (8).

The process is repeated by multiplying the second equation in (4) by u_0 , the third by u_1 and so on to the $(n + 2)$ nd equation which is multiplied by $u_n = 1$. This second modified set of $n + 1$ equations when added yields an equation the same as (9) except that $a + 1$ replaces a .

In a similar fashion, the process is repeated starting successively with the third, fourth, . . . and $(N-n)$ th equations to obtain the following set of equations, including (9):

$$\sum_{m=0}^{n-1} M(a + m + \ell) u_m = -M(a + n + \ell), \quad (10)$$

$$\ell = 0, 1, 2, \dots (N-n-1).$$

Since the set of $N-n$ equations in (10) is linear, it can be solved to obtain solutions for $u_0, u_1, u_2, \dots, u_{(n-1)}$. If $N = 2n$, then (10) contains n equations and n unknowns, and Crout's algorithm [Crout, 1941], or any other convenient method, may be used to obtain the solutions. In this case, the solutions are exact at the data points. However, if $N > 2n$, then (10) provides more equations than unknowns. All equations can be used by first reducing (10) to a set of n normal equations which in turn can be solved as described above. For the case $N > 2n$, the solutions obtained are a least-squares fit to the data points used.

When the n solutions for u_m have been obtained, then the Newton-Raphson or any other convenient method may be used to obtain the roots of (8), which are the n values of r_j . Temporary numerical subscripts are arbitrarily assigned to the solutions for r_j .

It can be seen that if the n solutions for r_j are substituted in (4), it becomes a set of N linear equations containing n unknown values of p_j . Any n equations of the set can then be solved to obtain the n solutions of p_j or, preferably, to improve the accuracy, the set of N linear equations can be reduced to a set of n normal equations that are solved to obtain the values of p_j . The numerical subscripts of p_j are determined by those previously assigned to r_j .

The method which has just been described for obtaining the solutions of p_j and r_j is used for each combination of antenna orientation and axis of measurement for which recorded data is obtained.

3.2. Matching and Averaging of Multiple Solutions

In obtaining the solutions for p_j and r_j , the assignment of numerical subscripts identifying the multipath components was arbitrary for each combination of antenna orientation and axis of measurement. Therefore, the subscripts are not in proper agreement between the solutions for one combination of antenna orientation and axis of measurement and those of another combination. It is necessary, then, to assign permanent numerical subscripts to each of the parallel sets of solutions so that all solutions with a given numerical subscript are actually describing the same multipath component. A description of how this can be done will be given with the aid of table 1.

Table 1 is composed of three major rows and three major columns for tabulated solutions of p_j and r_j . The three major rows represent the three antenna orientations and the three major columns are for the three axes of measurement that are used. The computed solutions for p_j and r_j , for each of the combinations of antenna orientation and axis of measurement that is used, are entered in the appropriate columns and rows. In the example of table 1 the numerical solutions, represented by dashes, are entered for all nine combinations of antenna orientation and axis of measurement.

Permanent numerical subscripts are initially assigned to the quantities in one box (major row and column) arbitrarily; in the table this was done for the box containing the x-axis measurements with the antenna parallel to the x axis. Then, since

$$p'_{xj} = p'_{yj} = p'_{zj}, \quad (11)$$

the numerical subscripts can be determined for the quantities in the other

two boxes in the same row by matching values of p_j of nominally the same value. If the assignment of numerical subscripts is started in the second or third major rows, (11) will still apply with a suitable change in the superscripts.

Permanent numerical subscripts can be assigned in the two remaining rows by major column by noting that

$$r'_{xj} = r''_{xj} = r'''_{xj} \quad (12)$$

and by matching nominally equal values of r_{xj} in the first column. Values in the second and third major columns can be matched in the same manner with a suitable change in the x subscript in (12).

When the assignment of subscripts is completed in all three major columns, (11) or its modifications can be used as a cross-check on the subscript assignment for the second and third major rows.

In order to insure that all spatial components of all multipath components are measured, and to allow the directions of arrival, α_j and β_j , for each multipath component to be determined unambiguously, it is necessary to place the restriction that each antenna orientation and each axis of measurement be used at least once in the measurements. This requires that solutions for p_j and r_j be obtained for at least three diagonally-located boxes in table 1. In addition, in order to properly assign permanent numerical subscripts, it is necessary to obtain measurements for a minimum of two additional boxes. Then, as mentioned earlier, a minimum of five combinations of antenna orientation and axis of measurement must be used.

An example of how numerical subscripts can be assigned in table 1 with five boxes of data is as follows: Let $x, y,$ and z designate the columns in table 1 and $'$, $''$, and $'''$ the rows. Assignment of subscripts can then be made to the following boxes in order: x', y', z', y'', z'' , and z''' , using (11) and

(12) or modifications of them. Of course, different groups of five are possible. It should be noted, however, that no cross-checking of the subscript assignment is possible with five boxes. If six boxes are used, cross-checking is possible; for example, if z' is added to the sequence above, then z' can be checked against the starting subscript assignments in x' . Any additional boxes over six for which data is obtained will allow more cross-checking, which is desirable to circumvent the difficulties which may occur because of faulty or inaccurate measurements.

While the hypothetical illustration of table 1 assumed that the same number of multipath components were measured for each combination of antenna orientation and axis of measurement, this may not always be the case. There are three field conditions which can occur to make the number of components measured differ between the combinations of antenna orientation and axis of measurement:

(a) If for any path of arrival a multipath component is linearly polarized in a direction parallel to the x - y , y - z , or x - z planes, it will produce no response in the second antenna for one antenna orientation. For measurements using that orientation, then, there will be one less component measured.

(b) If an elliptically-polarized multipath component has a path of arrival that coincides with any of the three axes of measurement, the moving dipole antenna will have no response when it is oriented parallel to that axis, resulting in one less component being measured for measurements using that antenna orientation.

(c) If the paths of arrival of two multipath components have equal angles of arrival with respect to one axis, even though the angle between the paths is large, measurements on that axis will see the two components as one, and measure them as such.

The probability that any of the above three conditions will exist under practical conditions is small. However, if any do occur, they must be considered in assigning permanent subscripts in table 1, and in subsequent calculations.

If condition (a) or (b) occurs it will be evidenced by the fact that the number of measured components in one major row of table 1 will be less than the number of components in the other two major rows. Which of the two conditions has occurred can be determined from an examination of the values of r_j (which contain the angles of arrival γ_j) for the "extra" component in the other two major rows. In either case, zero quantities can be entered for the "missing" p_j quantity, with a blank space for the companion r_j quantity.

If condition (c) occurs it will be evidenced by the fact that the number of measured components will be lower for one major column than for the other two columns. In this case, the simplest procedure is to discard the p_j quantity which represents the two combined multipath components and, in subsequent computations, use only the corresponding quantities in the other two major columns. However, the r_j quantity containing the two identical angles of arrival should be retained for subsequent computation of α_j and β_j .

The quantities which have been obtained for p_j and r_j provide a redundancy of information because of the requirement of five or more combinations of antenna orientation and axis of measurement. In the general case, if all nine combinations are used, values of p_j and r_j that are nominally identical are each obtained three times. These results can be averaged at this point in order to improve the accuracy of the figures used in subsequent computations. In obtaining averages it is desirable

to weight the redundant quantities in accordance with some estimate of their probable accuracies. While it is not practical to determine all of the factors in measurement and computation that influence the accuracies, it is quite certain that accuracies of the values obtained for p_j and r_j increase with the absolute value of p_j .

Since the values of p_j obtained from the three axes of measurement for any common antenna orientation are nominally the same, the equally-weighted average

$$p_j' = \frac{p_{xj}' + p_{yj}' + p_{zj}'}{3} \quad (13)$$

can be used. With a suitable change in the superscripts, (13) can be used to obtain the average values of p_j'' and p_j''' .

While the values of r_j obtained from one axis of measurement for three antenna orientations are nominally the same, their probable accuracy is not the same since the corresponding values of p_j are generally different. It is reasonable then to use the linearly-weighted average

$$r_{xj} = \frac{|p_{xj}'| r_{xj}' + |p_{xj}''| r_{xj}'' + |p_{xj}'''| r_{xj}'''}{|p_{xj}'| + |p_{xj}''| + |p_{xj}'''|} \quad (14)$$

which, with a suitable change in the subscripts, can be used to obtain values of r_{yj} and r_{zj} .

It follows from (6) and (7) then that

$$V_j' = \left[\operatorname{Re}^2(p_j') + \operatorname{Im}^2(p_j') \right]^{\frac{1}{2}}, \quad 0 \leq V_j' \quad (15)$$

$$\theta_j' = \tan^{-1} \left[\frac{\operatorname{Im}(p_j')}{\operatorname{Re}(p_j')} \right], \quad -\pi \leq \theta_j' \leq \pi \quad (16)$$

$$\bar{\sigma}_{xj} = -\frac{1}{2d} \ln \left[\operatorname{Re}^2(r_{xj}) + \operatorname{Im}^2(r_{xj}) \right], \quad (17)$$

and

$$\bar{\gamma}_{xj} = \cos^{-1} \left\{ \frac{\lambda}{2\pi d} \tan^{-1} \left[\frac{\operatorname{Im}(r_{xj})}{\operatorname{Re}(r_{xj})} \right] \right\}, \quad 0 \leq \gamma_{xj} \leq \pi \quad (18)$$

where the bars on $\bar{\sigma}_{xy}$ and $\bar{\gamma}_{xj}$ indicate the solutions contain errors to be corrected.

With suitable changes in the superscripts or subscripts in (15) through (18), values for V_j'' , V_j''' , θ_j'' , θ_j''' , $\bar{\sigma}_{yj}$, $\bar{\sigma}_{zj}$, $\bar{\gamma}_{yj}$, and $\bar{\gamma}_{zj}$ can be obtained.

3.3. Combined Solution

The angle of arrival of the j th multipath component with respect to the x axis, γ_{xj} , defines a cone whose axis is the x axis and one of whose elements is the path of arrival SO in fig. 2. Similarly, γ_{yj} and γ_{zj} define y - and z -axis cones, one element of each being the path SO. Ideally, then, the three cones intersect along a common line, the path of arrival SO.

However, because of errors in measurement, the angles of arrival obtained from the measurements, $\bar{\gamma}_{xj}$, $\bar{\gamma}_{yj}$, and $\bar{\gamma}_{zj}$, in general will not define cones that intersect along a common line. In most cases the measured cones will intersect along three closely spaced but different lines, one line for each combination of two cones. In some cases one or two of the combinations of cone pairs may fail to intersect at all. Because of the condition that the cones defined by the measured angles of arrival usually define several closely-spaced paths of arrival, it is desirable to obtain an average or best path of arrival based upon the several obtained.

The three types of discrepancy in the lines of intersection of the three cones of arrival are illustrated in fig. 3. Each of the three illustrations shows a small portion of the surface of a sphere which is centered on the origin of the coordinate system. Each small area illustrated is in the region where the lines of cone intersection pass through the surface of the sphere.

Fig. 3-a illustrates the most common case where all three pairs of cones intersect. It is the most common since it would usually occur for all paths of arrival that are not close to the x-y, y-z or x-z planes. Fig. 3-b illustrates the case which might occur if the path of arrival is close to one of the planes, where one pair of cones fails to intersect. Fig. 3-c illustrates the case where two pairs of cones fail to intersect; this might occur if the path of arrival is near one of the axes of the coordinate system.

It is desired to find a best point of intersection, I, based upon the values of $\bar{\gamma}_{xj}$, $\bar{\gamma}_{yj}$, and $\bar{\gamma}_{zj}$, for all three cases illustrated in fig. 3. Since the accuracy with which the three angles of arrival are determined is in general not equal, it is desirable to weight the values of $\Delta\gamma_{xj}$, $\Delta\gamma_{yj}$, and $\Delta\gamma_{zj}$ according to an estimate of the accuracies of $\bar{\gamma}_{xj}$, $\bar{\gamma}_{yj}$, and $\bar{\gamma}_{zj}$ respectively. The accuracy with which each of these angles can be determined can

be shown by differentiating (1) with respect to the angle of arrival of one of the multipath components, γ_{xj} , and modifying the result by (2) and (5) to obtain

$$\frac{\partial M_x(k)}{\partial \gamma_{xj}} = \frac{2\pi d}{i\lambda} k p_{xj} r_{xj}^k \sin \gamma_{xj} \quad . \quad (19)$$

It can be seen that the change in the angle of arrival that is required to change a single measurement by an amount comparable to the errors of measurement is inversely proportional to $p_{xj} \sin \gamma_{xj}$ and is a function of the position of measurement, k . Conversely, then, the errors in the measurements obtained for all of the values of k that are used will combine to produce an error in the computed value of γ_{xj} that is inversely proportional to $p_{xj} \sin \gamma_{xj}$, as well as directly proportional to the size of the errors of measurement. The accuracy of $\bar{\gamma}_{xj}$ is then directly proportional to $p_{xj} \sin \gamma_{xj}$. The effect of p_{xj} on the accuracy of $\bar{\gamma}_{xj}$ has already been considered in (14) and (18), which leaves only $\sin \gamma_{xj}$ to be considered in weighting the value of $\Delta \gamma_{xj}$. Similarly, $\sin \gamma_{yj}$ and $\sin \gamma_{zj}$ should be used to weight $\Delta \gamma_{yj}$ and $\Delta \gamma_{zj}$.

Therefore, to obtain the point I in fig. 3, let

$$S_j^2 = \left(\Delta \gamma_{xj} \sin \bar{\gamma}_{xj} \right)^2 + \left(\Delta \gamma_{yj} \sin \bar{\gamma}_{yj} \right)^2 + \left(\Delta \gamma_{zj} \sin \bar{\gamma}_{zj} \right)^2, \quad (20)$$

and let I be defined as that point for which (20) is a minimum. It can be shown that this occurs when

$$\Delta \gamma_{xj} \approx \epsilon_j \cot \bar{\gamma}_{xj}, \quad (21)$$

where

$$\epsilon_j = \frac{1}{4} \left(\cos 2\bar{\gamma}_{xj} + \cos 2\bar{\gamma}_{yj} + \cos 2\bar{\gamma}_{zj} + 1 \right). \quad (22)$$

With a suitable change in the x subscripts in (21), it applies also for $\Delta\gamma_{yj}$ and $\Delta\gamma_{zj}$.

The averaged value for the angle of arrival with respect to the x axis is then

$$\gamma_{xj} \approx \bar{\gamma}_{xj} + \Delta\gamma_{xj}, \quad (23)$$

which, with a suitable change in the x subscript, determines γ_{yj} and γ_{zj} .

The identity

$$\cos^2 \gamma_{xj} + \cos^2 \gamma_{yj} + \cos^2 \gamma_{zj} = 1 \quad (24)$$

can be used to test the accuracy of the solutions of (23). Because (21) is an approximation, the three solutions of (23) will have residual second-order errors which make them inconsistent with (24). A convenient method of avoiding the inconsistency is to obtain solutions from (23) for the two most accurate angles of arrival, those with the two largest sines, and to use these in (24) to obtain a consistent third angle.

It should be noted that while the accuracies with which the angles of arrival $\bar{\gamma}_{xj}$, $\bar{\gamma}_{yj}$, and $\bar{\gamma}_{zj}$ can be determined are dependent upon the sines of their values, the accuracy with which γ_{xj} , γ_{yj} , and γ_{zj} are obtained is independent of their values because of the weighting in (20); i. e., the accuracy of the angle of arrival of a multipath component is independent of its direction of propagation.

It follows, from the geometry of fig. 2, that the azimuthal and elevation angles of arrival are

$$\alpha_j = \tan^{-1} \left(\frac{\cos \gamma_{xj}}{\cos \gamma_{yj}} \right), \quad -\pi \leq \alpha_j \leq \pi \quad (25)$$

and

$$\beta_j = \left(\frac{\pi}{2} - \gamma_{zj} \right), \quad -\frac{\pi}{2} \leq \beta_j \leq \frac{\pi}{2}. \quad (26)$$

From the geometry of fig. 2, the rate of attenuation of the j th multipath component along the path SO can be determined from

$$\sigma_j = \frac{\sigma_{xj}}{\cos \gamma_{xj}} = \frac{\sigma_{yj}}{\cos \gamma_{yj}} = \frac{\sigma_{zj}}{\cos \gamma_{zj}}. \quad (27)$$

However, because of the errors of measurement, the values of $\bar{\sigma}_{xj}$, $\bar{\sigma}_{yj}$, and $\bar{\sigma}_{zj}$ if used in (27) will give inconsistent solutions. It is desirable, therefore, to correct these inconsistencies. Since the probable accuracies of the solutions from (17) are dependent upon the angles of arrival γ_{xj} , γ_{yj} , and γ_{zj} , it is reasonable to weight the individual solutions in (27) by the cosines of the angles of arrival to obtain the average solution

$$\sigma_j = \frac{\bar{\sigma}_{xj} \cos \gamma_{xj} + \bar{\sigma}_{yj} \cos \gamma_{yj} + \bar{\sigma}_{zj} \cos \gamma_{zj}}{\cos \gamma_{xj} + \cos \gamma_{yj} + \cos \gamma_{zj}}. \quad (28)$$

The solutions of (28) can then be used in (27) to obtain σ_{xj} , σ_{yj} , and σ_{zj} if they are desired.

The electric field components E^I_j , E^{II}_j , and E^{III}_j can be determined from the dipole pattern equation for the second antenna

$$E^I_j = CV^I_j \left[\frac{\sin \gamma_{xj}}{\cos\left(\frac{\pi}{2} \cos \gamma_{xj}\right)} \right], \quad (29)$$

which applies for E^{II}_j and E^{III}_j with the proper changes in the subscripts and superscripts. The coefficient, C , in (29) is a calibration constant.

The time phases determined with (16) are also the time phases of the electric field components because the dipole is at resonance and introduces no phase shift between an electric field component and its corresponding voltage component delivered by the antenna. Even if the dipole introduced a phase shift, it could be neglected since the phase shift would be the same for all components.

The values which have been obtained for E'_j , E''_j , E'''_j , θ'_j , θ''_j , and θ'''_j can be used to describe the j th multipath component in the more useful terms of $E_{\alpha j}$, $E_{\beta j}$, $\theta_{\alpha j}$, and $\theta_{\beta j}$. The relationships are defined by the following set of three equations based upon the geometry of fig. 2:

$$\begin{bmatrix} \cos \mu_{1j} & -\sin \mu_{1j} \\ \cos \mu_{2j} & \sin \mu_{2j} \\ 0 & 1 \end{bmatrix} \begin{bmatrix} E_{\alpha j} e^{i\theta_{\alpha j}} \\ E_{\beta j} e^{i\theta_{\beta j}} \end{bmatrix} = \begin{bmatrix} E'_j e^{i\theta'_j} \\ -E''_j e^{i\theta''_j} \\ E'''_j e^{i\theta'''_j} \end{bmatrix}, \quad (30)$$

where

$$\cos \mu_{1j} = \frac{\cos \gamma_{yj}}{\sin \gamma_{xj} \sin \gamma_{zj}}, \quad (31)$$

$$\sin \mu_{1j} = \frac{1}{\tan \gamma_{xj} \tan \gamma_{zj}}, \quad (32)$$

$$\cos \mu_{2j} = \frac{\cos \gamma_{xj}}{\sin \gamma_{yj} \sin \gamma_{zj}}, \quad (33)$$

and

$$\sin \mu_{2j} = \frac{1}{\tan \gamma_{yj} \tan \gamma_{zj}}. \quad (34)$$

Since there are three complex equations in (30) with two complex unknowns, any two of the equations can be used to obtain solutions. However, since the probable accuracy of the three equations in general is not the same, it is desirable to weight the equations in accordance with some estimate of the probable accuracies, and then use all three to obtain a least-squares solution.

The accuracy of the first equation in (30) is dependent upon the accuracy of E'_j , and therefore V'_j . Since the accuracy of $V'_j = |p'_j|$ was earlier assumed to be proportional to its value, it is reasonable to weight the first equation in (30) by V'_j . The second and third equations then should be weighted by V''_j and V'''_j , respectively. When so weighted, (30) reduces to the following set of normal equations:

$$\begin{bmatrix} \left(V'_j \cos^2 \mu_{1j} \right) & \left(-\frac{1}{2} V'_j \sin 2\mu_{1j} \right) \\ + V''_j \cos^2 \mu_{2j} & + \frac{1}{2} V''_j \sin 2\mu_{2j} \end{bmatrix} \begin{bmatrix} E_{\alpha j} e^{i\theta_{\alpha j}} \\ E_{\beta j} e^{i\theta_{\beta j}} \end{bmatrix} = \begin{bmatrix} \left(V'_j \cos \mu_{1j} E'_j e^{i\theta'_j} \right) \\ - V''_j \cos \mu_{2j} E''_j e^{i\theta''_j} \\ - V'_j \sin \mu_{1j} E'_j e^{i\theta'_j} \\ + V''_j \sin \mu_{2j} E''_j e^{i\theta''_j} \\ + V'''_j E'''_j e^{i\theta'''_j} \end{bmatrix} \quad (35)$$

Equation (35) can be solved by any convenient method to obtain solutions for $E_{\alpha j}$, $E_{\beta j}$, $\theta_{\alpha j}$, and $\theta_{\beta j}$ which, with those obtained from (25), (26), and (27), provide the desired final solutions.

3.4. Rotation of the Coordinate System

In the preceding analysis of the aperture synthesis method of measuring a multipath field, it was assumed that the coordinate system was oriented to make the x-y plane horizontal, as shown in fig. 2. This assumption was made to simplify the description. However, there is another orientation of the coordinate system which is superior for practical reasons, an orientation where each of the three orthogonal axes of measurement forms the same angle with respect to a horizontal plane, as shown in fig. 4. In fig. 4 the dashed lines are the x, y, and z axes of measurement, each of which forms an angle of 35.26° with respect to the horizontal X-Y plane. This orientation of the axes of measurement is advantageous because it is mechanically simpler to construct and operate a track and moving antenna system which can be moved from one axis of measurement to another, and/or from one antenna orientation to another.

If the orientation of the x-y-z coordinate system of fig. 4 is used rather than that of fig. 2, it is necessary to extend the analysis of the preceding sections to obtain the final solutions with respect to the X-Y-Z coordinate system. E_{A_j} , E_{B_j} , θ_{A_j} , θ_{B_j} , A_j , and B_j are obtained in place of their analogous counterparts E_{α_j} , E_{β_j} , θ_{α_j} , θ_{β_j} , θ_{β_j} , α_j , and β_j , and are defined with respect to the X-Y-Z coordinate system in the same way their counterparts were defined with respect to the x-y-z coordinate system. The distance-decay factor, σ_j , is independent of the rotation of the coordinate system.

The relationships between the components of the two coordinate systems is illustrated in fig. 5. It is based upon a double rotation of the x-y-z coordinate system to make it coincide with the X-Y-Z system.

By this analysis it can be shown that

$$A_j = \tan^{-1} \left(\sqrt{3} \frac{\cos \gamma_{xj} - \cos \gamma_{zj}}{-\cos \gamma_{xj} + 2 \cos \gamma_{yj} - \cos \gamma_{zj}} \right), \quad -\pi \leq A_j \leq \pi \quad (36)$$

$$B_j = \sin^{-1} \left(\frac{\cos \gamma_{xj} + \cos \gamma_{yj} + \cos \gamma_{zj}}{\sqrt{3}} \right), \quad -\frac{\pi}{2} \leq B_j \leq \frac{\pi}{2} \quad (37)$$

$$E_{A_j} = \left[\begin{array}{c} E_{\alpha_j}^2 \cos^2 \rho_j + E_{\beta_j}^2 \sin^2 \rho_j \\ - E_{\alpha_j} E_{\beta_j} \sin 2\rho_j \cos(\theta_{\alpha_j} - \theta_{\beta_j}) \end{array} \right]^{\frac{1}{2}}, \quad 0 \leq E_{A_j} \quad (38)$$

$$E_{B_j} = \left[\begin{array}{c} E_{\alpha_j}^2 \sin^2 \rho_j + E_{\beta_j}^2 \cos^2 \rho_j \\ + E_{\alpha_j} E_{\beta_j} \sin 2\rho_j \cos(\theta_{\alpha_j} - \theta_{\beta_j}) \end{array} \right]^{\frac{1}{2}}, \quad 0 \leq E_{B_j} \quad (39)$$

$$\theta_{A_j} = \tan^{-1} \left(\frac{E_{\alpha_j} \sin \theta_{\alpha_j} \cos \rho_j - E_{\beta_j} \sin \theta_{\beta_j} \sin \rho_j}{E_{\alpha_j} \cos \theta_{\alpha_j} \cos \rho_j - E_{\beta_j} \cos \theta_{\beta_j} \sin \rho_j} \right), \quad (40)$$

$$-\pi \leq \theta_{A_j} \leq \pi$$

and

$$\theta_{B_j} = \tan^{-1} \left(\frac{E_{\alpha_j} \sin \theta_{\alpha_j} \sin \rho_j + E_{\beta_j} \sin \theta_{\beta_j} \cos \rho_j}{E_{\alpha_j} \cos \theta_{\alpha_j} \sin \rho_j + E_{\beta_j} \cos \theta_{\beta_j} \cos \rho_j} \right), \quad (41)$$

where

$$\rho_j = \tan^{-1} \left[\sqrt{\frac{2}{3}} \frac{\left(1 - \cos \gamma_{xj} \cos \gamma_{yj} - \cos \gamma_{xj} \cos \gamma_{zj} - \cos \gamma_{yj} \cos \gamma_{zj} \right)^{\frac{1}{2}} (\cos \gamma_{yj} - \cos \gamma_{xj})}{\left(1 - \cos^2 \gamma_{zj} - \cos \gamma_{yj} \cos \gamma_{zj} - \cos \gamma_{xj} \cos \gamma_{zj} \right)} \right] \quad (42)$$

$$-\pi \leq \rho_j \leq \pi$$

4. Discussion

From the preceding analysis it can be seen that the aperture-synthesis method of measuring a multipath field that has been described consists of two parts: (a) obtaining preliminary parallel solutions for p_j and r_j from the measurements for each combination of antenna orientation and axis of measurement used, and (b) obtaining final solutions from the preliminary solutions. If preliminary solutions of sufficient accuracy can be obtained so that they can be properly matched for the assignment of numerical subscripts, then obtaining final solutions should pose no difficulty. Therefore, the practicality of the method is dependent upon whether or not preliminary parallel solutions of sufficient accuracy can be obtained to allow for their proper matching.

The question arises as to whether or not a priori knowledge of the number of multipath components is necessary in order to obtain preliminary solutions. If the elements of the M matrix of (10) are replaced by their respective functions of p_j and r_j in (4) for the cases where $n = 2$ and $n = 3$, it can be shown that the values of the M determinant are

$$\Delta_M = -p_1 p_2 (r_1 r_2)^a (r_1 - r_2)^2, \quad n = 2 \quad (43)$$

$$\Delta_M = -p_1 p_2 p_3 (r_1 r_2 r_3)^a (r_1 - r_2)^2 (r_1 - r_3)^2 (r_2 - r_3)^2, \quad n = 3. \quad (44)$$

Then it reasonably can be assumed that for the general case

$$\Delta_M = \sqrt{2} \sin \left[\frac{\pi}{4} (2n+1) \right] \prod_{j=1}^n \prod_{i=j+1}^n p_j r_j^a (r_j - r_i)^2. \quad (45)$$

Because the sign of the determinant is not important in the discussion that follows, a justification for the sinusoidal function that determines it will not be given.

It appears at first consideration of (45) that if the assumed number of multipath components, n , were greater than the actual number in the measured field, n_a , that $n-n_a$ of the factors p_j would be zero. The resulting M determinant would likewise be zero and result in indeterminate solutions for the n values of u_m in (10). In turn, this would prevent solutions for r_j and p_j from being obtained. This seems to indicate that a priori knowledge of the number of multipath components is necessary.

Actually, however, this is not the case. In any practical measurement of a field, the measurements will have some degree of error, i. e., the values of $M(k)$ will have a limited number of significant figures. If zeros are appended to each of these measurements, to make them appear as if they had more significant figures, then Δ_M will not be zero and solutions can be obtained. The reason for this is that the errors in the measurements in effect introduce fictitious multipath components with amplitudes comparable to the size of the errors. With the addition of zeros to the measurements, the resulting precision of the computations can be made arbitrarily high so that solutions can be obtained for the $n-n_a$ fictitious components as well as for the n_a actual components. This is true regardless of the accuracy of the measurements, it only being necessary to carry several more significant figures in the computations than are present in the measurements. The extra fictitious component solutions obtained for any preliminary solution can be recognized and discarded since they will be weak and will not agree with those obtained for the other parallel solutions.

In general, then, it is possible to obtain solutions for the actual multipath components in a measured field, providing the assumed number of multipath components used in the computations is equal to or greater than the actual number of components of significant strength. Components

of significant strength are those whose amplitudes are in the order of or greater than the absolute errors of measurement. If the assumed number of multipath components is less than the actual number, then it is obvious that the solutions will be too few in number and can be greatly in error.

In a practical application of the aperture synthesis method, consideration must be given to the choice of the number of data points that are used to obtain solutions. Theoretically, there is no limit to the maximum number of data points that can be used; the number can be increased indefinitely by making the spacing between adjacent points of measurement, d , sufficiently small. On the other hand, the minimum number of data points that can be used is restricted in two ways:

- (a) At least $2n$ data points are necessary to obtain solutions.
- (b) If the aperture or distance over which measurements are made is D , then the minimum number of data points is $\frac{2D}{\lambda} + 1$, because adjacent data points cannot be spaced greater than $\lambda/2$ if multiple solutions of (18) are to be avoided.

Whether or not it is desirable to use the minimum number of data points or to use a larger number is dependent upon the comparative accuracies of the solutions. In general, two methods of obtaining solutions are possible:

- (a) Let $N = 2n$, in which case the function $M(k)$ in (4) defined by the solutions fits the measured values exactly at the points of measurement.
- (b) Let $N > 2n$, in which case the function $M(k)$ in (4) defined by the solutions is a least-squares fit to the measured values.

If method (a) is used to obtain solutions, and if the errors of measurement are random, then the accuracy of the solutions for the actual multipath components may improve as the number of data points increases. If method (b) is used to obtain solutions, and if the errors of measurement are random, then the accuracy of the solutions should definitely improve as the number of data points increases. However, in practical cases of

measurement, bias-type or other non-random errors are likely to occur and no general statement can be made concerning either the optimum number of data points or which of the two methods of obtaining solutions will yield the most accurate answers. In any case, the advantage of any improvement in accuracy which may result by using more data points must be weighed against the attendant disadvantage of the larger number of computations required.

It is of interest to consider the resolving capabilities of the aperture-synthesis method, i. e., what dynamic range of multipath signal strengths can simultaneously be measured, and how small can the angular separation between multipath components be without their appearing as one component in the solutions. Both are obviously limited by the accuracy of the measurements, the greater the accuracy of the measurements, the greater the dynamic range and the greater the angular resolving power.

Since errors of measurement can introduce fictitious solutions whose amplitudes are of the same order as the size of the errors, the weakest multipath components that can be detected and measured should be of this same order of amplitude. The dynamic range of the aperture-synthesis method should then be approximately equal to the ratio of the strongest component to the errors of measurement.

Since measurements are made along the coordinate axes over a distance D , the angular resolution reasonably can be expected to be approximately λ/D radians, the beamwidth of an antenna of equal aperture. It is probably not reasonable to expect much better resolving power than this without inordinately high accuracies of measurement, since the results would be equivalent to those obtained from a super-gain antenna of aperture D .

5. Experimental Results

In order to determine the practicality of the aperture-synthesis method of measuring a multipath field, an experimental evaluation program was undertaken. The program was composed of two parts: (a) a computer evaluation of the technique and (b) actual field measurements of a multipath field. Because of the quantity of computations that are needed to obtain solutions for the multipath components, a digital computer program was written to provide solutions in the experimental program.

In order to make a computer evaluation of the aperture-synthesis technique, a second computer program was written to generate hypothetical measurements. The quantities describing each of an arbitrary number of multipath components could be assumed for a hypothetical field from which the second program could generate measurements of V_b and ϕ to a high degree of accuracy for the different combinations of antenna orientation and axis of measurement. The "measurements" could then be fed to the first computer program to obtain solutions which could be compared with the originally assumed multipath values to determine the validity and accuracy of the technique. A variety of field conditions and accuracies of measurement of known magnitude could be easily simulated to determine their effects on the solutions.

As mentioned above, probably the most critical part of the aperture-synthesis method is that of obtaining preliminary parallel solutions of sufficient accuracy to allow proper identification of multipath components. For this reason, some of the initial tests in the computer evaluation program were made for only a single combination of antenna orientation and axis of measurement. The purposes of these tests were (a) to determine the effect of the accuracy of the measurements on the accuracy of the preliminary solutions, (b) to determine the dynamic range of signal

amplitudes for which solutions can be simultaneously obtained, and (c) to determine the angular resolution. These tests were made by Stearns and Chrisman [1963] using a hypothetical field of four multipath components ($n_a = 4$) with arbitrarily different amplitudes, phases, and angles of arrival, and zero distance-decay factors. Values used in obtaining solutions were $D = 9.5\lambda$, $d = \lambda/2$, and $n = N/2 = 10$.

In determining the effect of the accuracy of the measurements on the accuracy of the preliminary solutions, hypothetical measurements were generated for four multipath components whose amplitudes were distributed over a 7-dB range. The accuracy of the measurements was controlled by the number of significant figures that were used to obtain solutions. With three-figure accuracy in the measurements, the resulting solutions had average errors in amplitude, phase and angle of arrival of 0.018 dB, 0.21° , and 0.026° respectively. The average amplitude of the six fictitious solutions was 53.1 dB below the strongest actual component. With two-figure accuracy in the measurements, the solutions had average errors in amplitude, phase, and angle of arrival of 0.075 dB, 0.32° , and 0.11° respectively; the maximum errors were 0.091 dB, 0.62° , and 0.25° . With two-figure accuracy the average amplitude of the six fictitious solutions was 41.5 dB below that of the strongest component.

A dynamic range test was made by assuming the same four hypothetical multipath components except that the weaker of the four was made to have successively lower amplitudes. For each amplitude, hypothetical measurements were generated and solutions obtained using measurements with two-figure accuracy. The errors in the solutions for the amplitude, phase, and angle of arrival of the weakest, varied component were greater than those of the stronger multipath components. With the weakest component at a level 28 dB below that of the strongest, its errors in amplitude, phase, and angles of arrival were 1.82 dB, 11.2° , and 0.67°

respectively. At a level 40 dB down, the errors increased to 2.28 dB, 92.5°, and 10.9° respectively.

An angular resolution test was made by assuming the same four multipath components used in the test to determine the effect of the accuracy of the measurements on the accuracy of the preliminary solutions, except that the two weakest components were allowed to have a successively smaller difference in their angles of arrival. For each angular separation, measurements with two-figure accuracy were used to obtain solutions. It was found that as the angular separation decreased below the equivalent beamwidth of the aperture (λ/D radians or 6.0°), the errors increased rapidly. For an angular separation of 10° , the average errors in amplitude, phase, and angle of arrival for the two weak components were 0.045 dB, 1.46° , and 0.16° respectively. For an angular separation of 3° , the average of the errors increased to 4.18 dB, 10.4° , and 3.38° respectively.

In obtaining the previously quoted results, 20 data points were used to obtain solutions for an assumed 10 multipath components, 6 of which were fictitious. The resulting 10 solutions defined the function (4) which fit the measurements exactly at the 20 data points. Tests have not yet been made with more data points at closer spacing and/or a smaller number of assumed components in order to determine the relative performance of least-squares solutions.

Fig. 6 is a photograph of an experimental Fiberglas track and carriage which has been constructed for making measurements of multipath fields. A folded dipole antenna is mounted on the motor-driven carriage which is synchronized with a chart recorder. The 5.5-m track is supported at an angle of 35.26° with respect to a horizontal plane and can be rotated about the vertical column to provide three orthogonal axes of measurement. The column supporting the dipole can be rotated about its axis to provide the three orthogonal antenna orientations.

Using this track and carriage, Kilpatrick [1963] made measurements of a controlled multipath field. The multipath field was created by feeding the output of a single 400-Mc/s transmitter to two horizontally-polarized antennas, with a power-division ratio of four to one. The transmitting antennas were each 3 m above the ground and were separated in azimuth by 24.5° at the measuring site approximately 150 m away. Four multipath components were produced, two direct waves and two ground-reflection components. The angular separation between each pair of direct and ground-reflected components was about 2° . Measurements were obtained for all nine combinations of antenna orientation and axis of measurement using an aperture of 6λ , corresponding to a beamwidth or angular resolution of about 9.5° . The computer solutions obtained from the measurements yielded two significant components; the direct and ground-reflected components from each antenna appeared as one component because their angular separation was much smaller than the angular resolution. The two solutions had an angular separation of 22.8° , an error of 1.7° ; their elevation angles of arrival were 2.0° and 9.6° above the direct paths. The two solutions had an amplitude ratio of 1.9, in reasonable agreement with the transmitted amplitude ratio of 2.0. The vertical components for each solution were about 27 dB below the horizontal components. No test of the phase accuracy of the solutions was practical.

6. Conclusions

The analysis and results which have been presented show that field-strength measurements made with a small-aperture antenna that is moved along three orthogonal straight lines can be used to compute the numerical quantities that define each of a number of coherent elliptically-polarized multipath field components. The dynamic range of the amplitudes of the multipath field components that can be measured is approximately equal

to the ratio of the amplitude of the strongest component to the amplitude of the errors of measurement. The minimum angular separation which two multipath components may have without being seen as one component is approximately equal to the beamwidth of an antenna whose aperture is equal to the linear distance of movement of the measuring antenna. The magnitude of the errors in the solutions is least for the strongest multipath components and greatest for the weakest components; limited tests indicate that with measurements of two-figure accuracy the stronger-component errors are less than one-tenth of a dB in amplitude, several tenths of a degree in phase and about one-tenth of a degree in angle of arrival.

The great advantage of the aperture-synthesis method of measuring a multipath field over conventional methods of making field-strength measurements is that it is capable of measuring the individual multipath components which makes a much more detailed description of the field in the area of measurement possible. Its disadvantages are the greater time and complexity of the measurements, the limitation of its use to a field with a CW component, the unchanging-field conditions required during measurement and the subsequent computations that are required. For this reason it is likely to be most useful in applications where the advantage of a complete description of a multipath field outweigh the disadvantages of measuring complexity. Antenna-siting measurements or similar surveys are possible applications where the aperture-synthesis method may be used to advantage.

The primary purpose in undertaking the development of the aperture-synthesis method that has been described has been to investigate the basic feasibility of the aperture-synthesis technique. The use of a rotating antenna in place of an antenna that is moved along straight lines and other modifications may be possible that will improve the technique [Mittra and Stearns, 1964].

The author wishes to thank H. V. Cottony for his suggestion to investigate the aperture-synthesis approach to measuring multipath fields and to gratefully acknowledge the computer analysis of the method made by C. O. Stearns and M. E. Chrisman and the design of the track-and-carriage equipment and field measurements of E. L. Kilpatrick.

7. References

- Brooks, F. E. (1951), A receiver for measuring angle-of-arrival in a complex field, *Proc. IRE*, 39, 407-411.
- Crout, P. D. (1941), A short-method for evaluating determinants and solving systems of linear equations with real or complex coefficients, *Trans. AIEE*, 60, 1235-1240.
- Cottony, H. V. (1958), Techniques for accurate measurement of antenna gain, *NBS Circular* 598, 3.
- Hamlin, E. W., P. A. Seay, and W. E. Gordon (1949), A new solution to the problem of vertical angle-of-arrival of radio waves, *J. App. Physics*, 20, 251-258.
- Hildebrand, F. B. (1956), *Introduction to Numerical Analysis*, p. 378 (McGraw-Hill Book Co., Inc., New York, N.Y.).

- Kilpatrick, E. L. (1963), Private communication.
- Mitra, R., and C.O. Stearns (1964), Field strength measurements in a multipath field using linear and circular probing, Proc. Tenth-tri-Service Conf. on Electromagnetic Compatibility, Chicago, Ill., Nov. 17-19.
- Ryle, M. (1957), The Mullard Radio Astronomy Observatory, Cambridge, Nature, 180, 110-112.
- Ryle, M. (1960), The Mullard Radio Astronomy Observatory, J. Inst. Elec. Eng., 6, 14-18.
- Stearns, C. O., and M. E. Chrisman (1963), Private communication.
- Watterson, C. C. (1962), Field-strength measurements in a multipath field, Symposium Digest, 4th Nat. Symp. on Radio Freq. Interference, San Francisco, June 28-29.

		Axis of Measurement								
		x axis		y axis		z axis				
Antenna Parallel to	x axis	j	p'_{xj}	r'_{xj}	j	p'_{yj}	r'_{yj}	j	p'_{zj}	r'_{zj}
		1	-	-	2	-	-	3	-	-
		2	-	-	4	-	-	2	-	-
		3	-	-	3	-	-	4	-	-
	4	-	-	1	-	-	1	-	-	
	y axis	j	p''_{xj}	r''_{xj}	j	p''_{yj}	r''_{yj}	j	p''_{zj}	r''_{zj}
		2	-	-	4	-	-	1	-	-
		3	-	-	1	-	-	3	-	-
		4	-	-	3	-	-	2	-	-
	1	-	-	2	-	-	4	-	-	
	z axis	j	p'''_{xj}	r'''_{xj}	j	p'''_{yj}	r'''_{yj}	j	p'''_{zj}	r'''_{zj}
		3	-	-	4	-	-	3	-	-
2		-	-	3	-	-	2	-	-	
4		-	-	2	-	-	1	-	-	
1	-	-	1	-	-	4	-	-		

Table 1 - Tabulation of calculated values for assignment of numerical subscripts

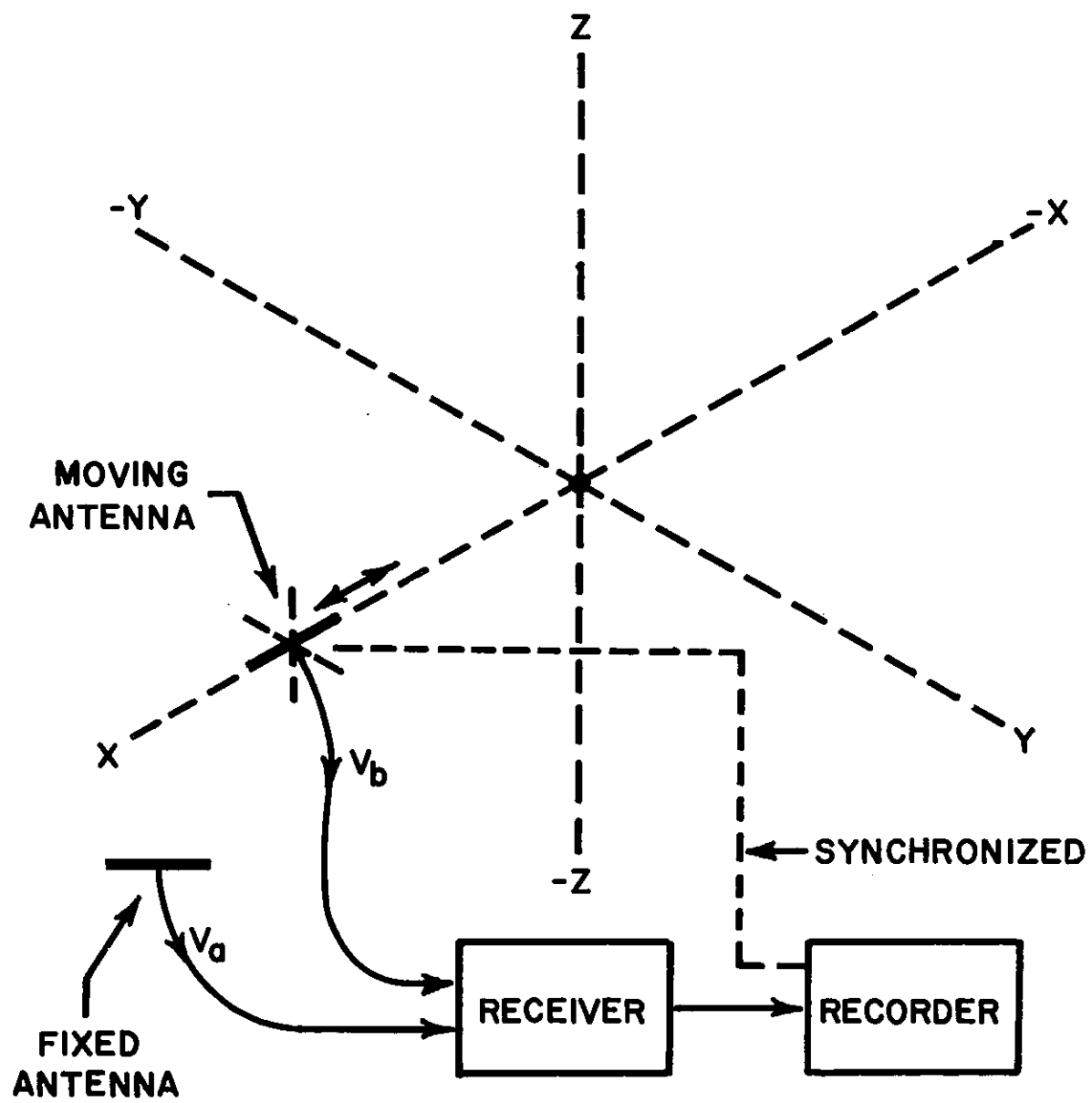


Figure 1. Arrangement of the measuring equipment.

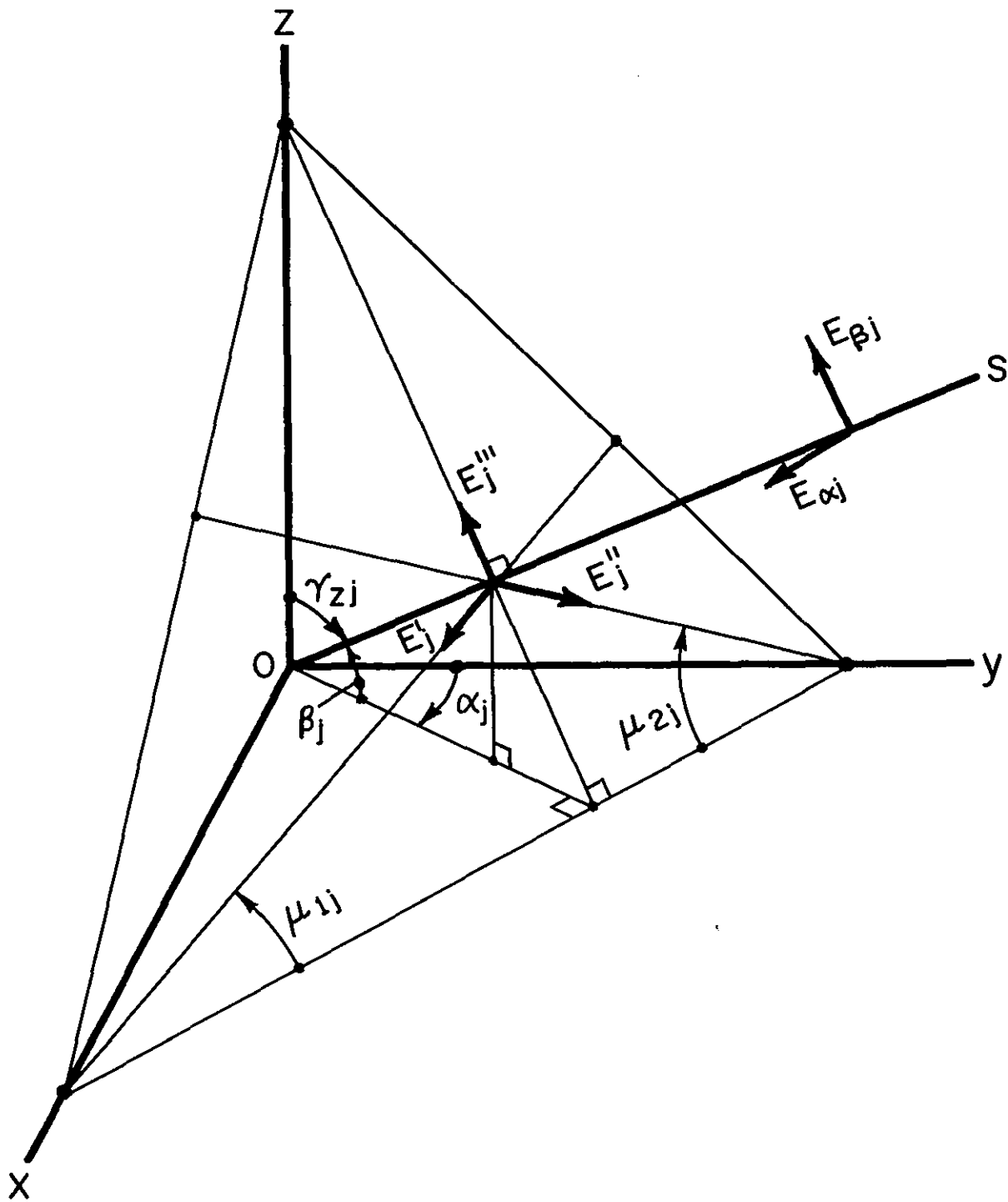


Figure 2. Relationship of the j th multipath component to the coordinate system.

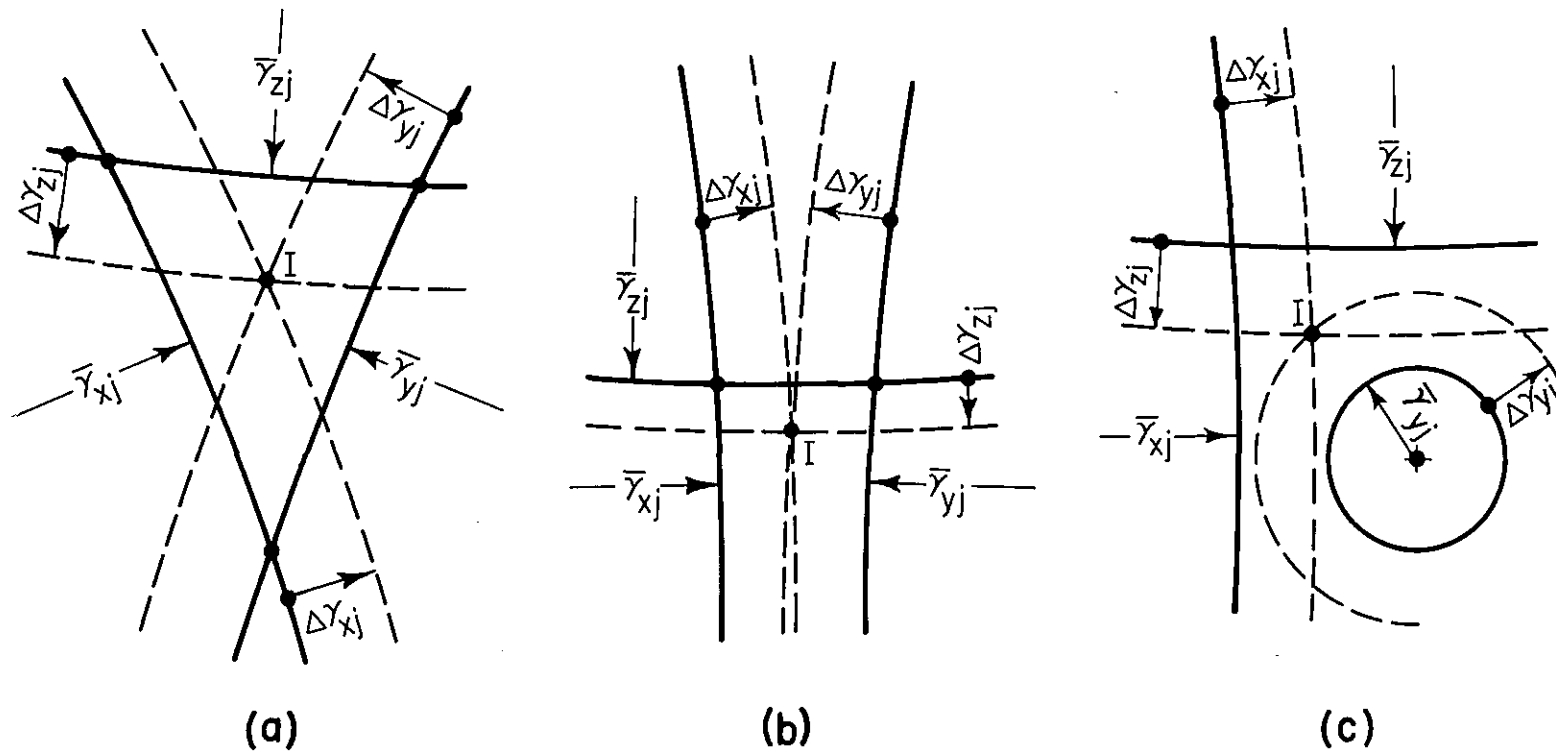


Figure 3. Discrepancies in the lines of intersection of the three cones of arrival.
 (a) All three combinations of cone pairs intersecting.
 (b) Two combinations of cone pairs intersecting.
 (c) One cone pair intersecting.

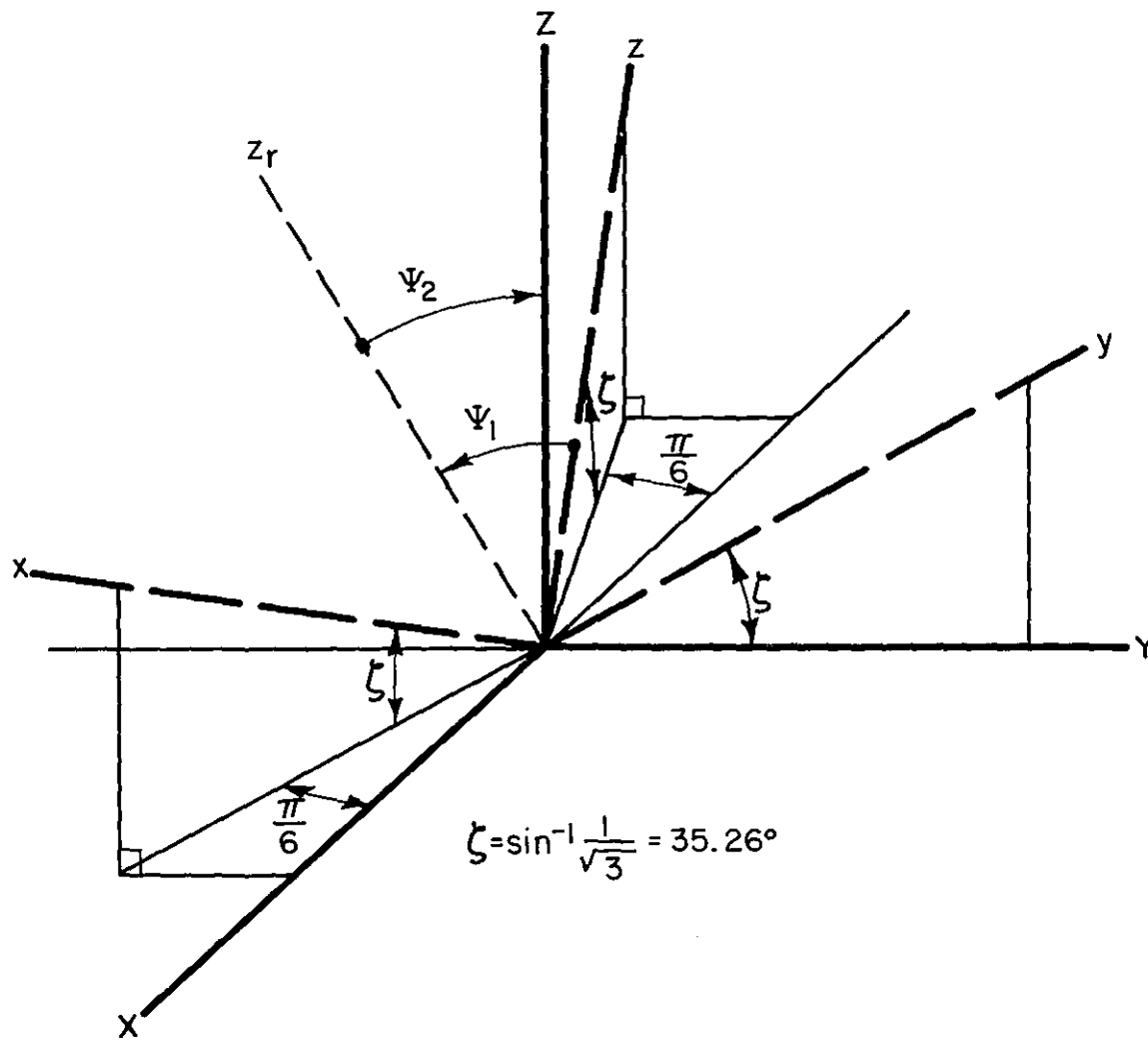


Figure 4. Preferred orientation of the x-y-z axes of measurement and their relationship to the X-Y-Z coordinate system.

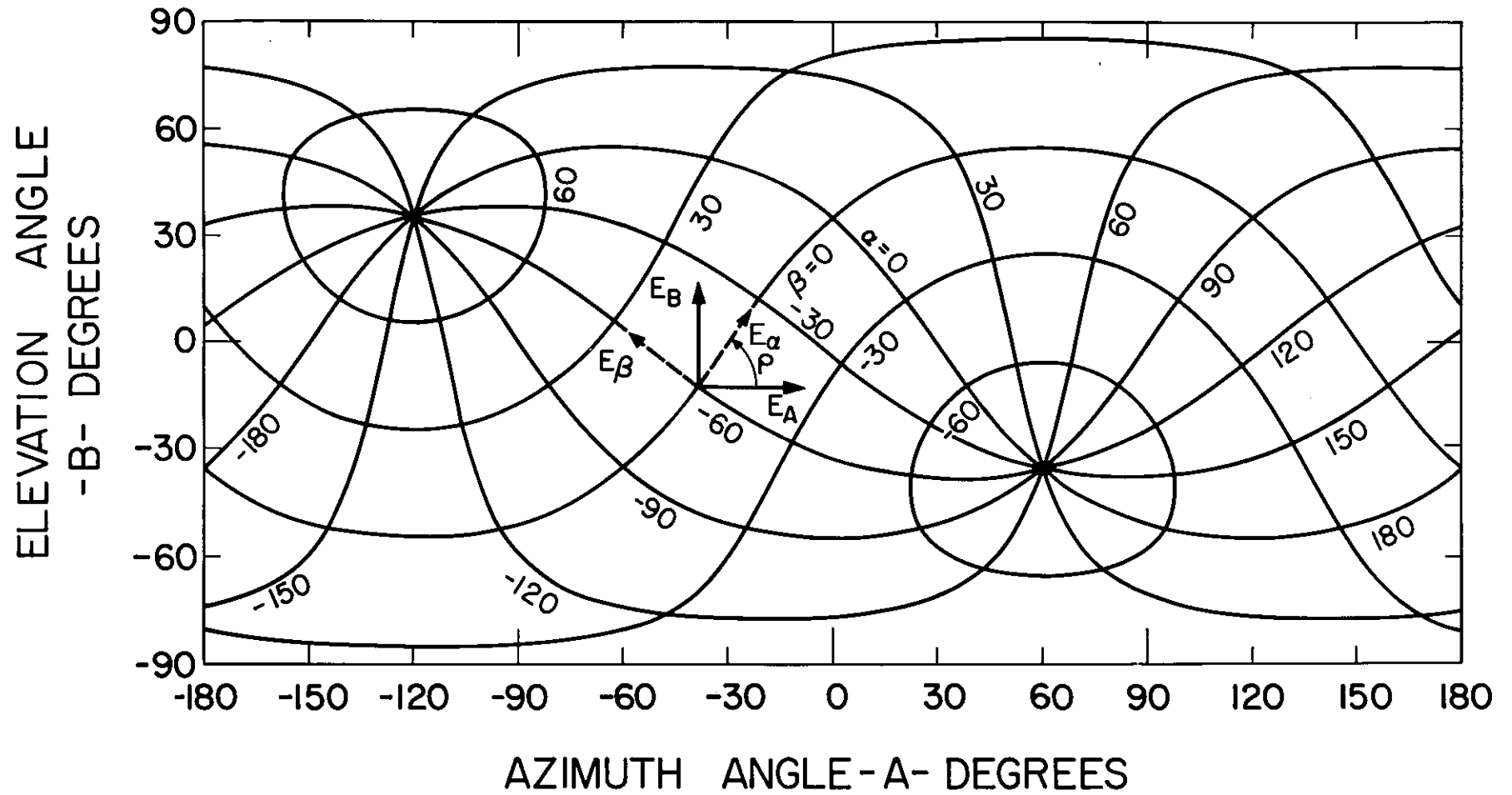


Figure 5. Relationship of the x-y-z coordinate system components to the X Y-Z coordinate system components.

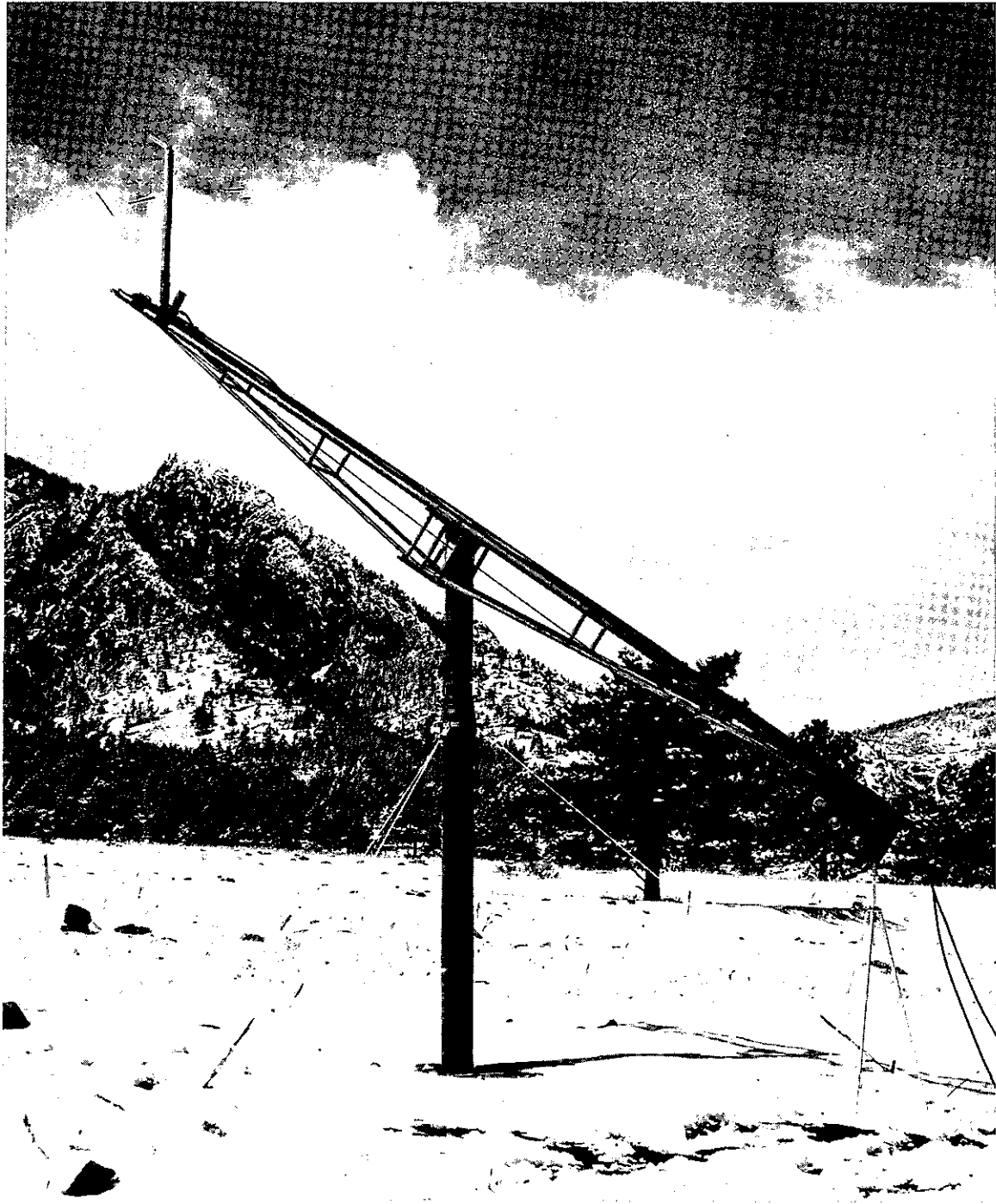


Figure 6. Experimental track and carriage.